All-optical microwave feedback oscillator with atomic cell resonator

R. Boudot,[1] M. Abdel Hafiz,[1] M.Petersen,[1] C. E. Calosso,[2] and E. Rubiola[1,2]
[1)] *FEMTO-ST, CNRS, Université Bourgogne Franche-Comté, Besançon, France*
[2)] *INRIM, Strada delle Cacce 91, Torino, Italy*

(*Electronic mail: rodolphe.boudot@femto-st.fr)

We report the demonstration of an all-optical self-sustained cell-based microwave feedback oscillator. In this scheme, a microwave resonance, optically-induced in a buffer-gas filled vapor cell resonator through coherent population trapping (CPT), is detected by a fast photodiode, amplified and used to drive back, through a frequency divider, a Mach-Zehnder electro-optic modulator in a sustaining loop configuration. The total gain and phase of the system was measured in open-loop configuration with a network analyzer. In good agreement with values predicted by the Leeson effect, the CPT feedback oscillator demonstrates an absolute phase noise of -24 dBrad^2/Hz at 1 Hz offset frequency, compatible with a fractional frequency stability of 8×10^{-12} at 1 s, and a phase noise floor of -112 dBrad^2/Hz, limited by the low microwave power available at the photodiode output. The amplitude noise of the oscillator shows a comparable noise floor and, for offset frequencies lower than 200 Hz, a $1/f$ dependence, due to the presence of the frequency divider in the loop.

Coherent population trapping (CPT)[1,2] is a quantum interference process in which atoms are optically pumped into a dark state by interacting with a dual-frequency laser field that connects two atomic ground states to a common excited state. The fulfillment of the null Raman detuning condition keeps the atoms in a coherent superposition of the two ground states with a typical relaxation time T_2. In buffer-gas vapor cell experiments, the microwave hyperfine coherence lifetime T_2 is usually in the 0.1 – 10 ms range, yielding ultimate atomic resonance linewidths $\Delta\nu = 1/(\pi T_2)$ in the 30 – 3000 Hz range (neglecting power broadening effects) and then Q-factors, if using Cs or Rb atoms, of 10^6 – 10^8. The exquisite properties of CPT resonances make them attractive candidates for a plethora of applications including laser spectroscopy[3], atomic frequency standards[4–8], sensors[9,10], slow-light experiments[11] or laser cooling[12].

Most CPT-based vapor cell atomic clocks operate as a passive atomic frequency standard[13]. In this case, the atomic resonance is probed by scanning the frequency of an optically-carried microwave signal delivered by a local oscillator (LO) and is detected with a slow photodiode as an increase of the light power transmitted through the vapor cell. A derivative error signal, crossing zero at the resonance extremum, is then obtained by probing both sides of the resonance and can be processed to stabilize the LO frequency onto the atomic frequency. An alternative approach, known as the CPT maser[14], consists to place the cell in an electromagnetic cavity in order to produce an oscillating magnetization responsible for the emission of a coherent signal emission at the atomic ground state hyperfine transition frequency. Other studies have demonstrated the possibility to directly detect, at the cell output with a fast photodiode, microwaves generated through stimulated Raman scattering (SRS)[15,16], electromagnetically-induced transparency (EIT)[15] or CPT[17–22]. These approaches have been used to phase-lock, to a microwave atomic cell frequency reference, neighboring modes of multi-mode[21] or current-modulated lasers[22], or to construct self-oscillating atomic cell oscillators[17–19,22].

In this paper, we investigate the unusual concept of a CPT-based vapor cell atomic feedback oscillator[17–19], comparable in its architecture to those of opto-electronic oscillators (OEOs)[23,24], with the fiber delay line being replaced by the alkali vapor cell. In our setup, a high-Q atomic resonance, initiated through CPT in a buffer-gas filled Cs vapor cell, is detected with a fast photodiode, amplified and sustained in a loop oscillator configuration, by driving back through a frequency divider, a diode laser modulated with a fibered Mach-Zehnder electro-optic modulator (EOM). The latter is driven at half of the clock transition frequency and biased at its dark point, such that a proper CPT-resonant dual-frequency optical field, free from excess sidebands, is generated by both first-order optical sidebands. For better understanding of actual limitations of the cell-based feedback oscillator, a simple and straightforward phase noise metrology analysis is used. The phase noise of the Cs cell atomic oscillator is -24 dBrad^2/Hz at f = 1 Hz, compatible with a frequency stability of 8×10^{-12} at 1 s, and -112 dBrad^2/Hz at f = 10 kHz. These results, at least one order of magnitude better than those previously-reported by atomic cell-based OEOs, are in good agreement with the Leeson model[25,26]. The amplitude modulation (AM) noise of the oscillator was also measured, showing a comparable floor level and flicker of amplitude dependence for $f < 200$ Hz.

Figure 1 presents the experimental setup. The optical setup used for this study was mainly extracted from the existing one described in Ref.[7]. The heart of the experiment is a 2-cm diameter and 5-cm long buffer-gas filled (N_2-Ar mixture) Cs vapor cell. The cell is maintained in a temperature-stabilized physics package that also integrates a solenoid, for optional application of a static magnetic field parallel used to raise the Zeeman degeneracy. This ensemble is surrounded by a double-layer mu-metal magnetic shield. In the present study, most of the experiments were performed at null magnetic field. These conditions were found to be favorable for increasing the atomic signal and subsequently improve the oscillator phase noise performances. A CPT atomic resonance can be created in the cell by making the atoms interact with a dual-frequency optical field. For this purpose, we use a Distributed Feedback (DFB) diode laser, tuned on the Cs D_1 line at 894.6 nm, externally-modulated by a fibered Mach-Zehnder electro-optic modulator (EOM), ultimately driven by the feed-

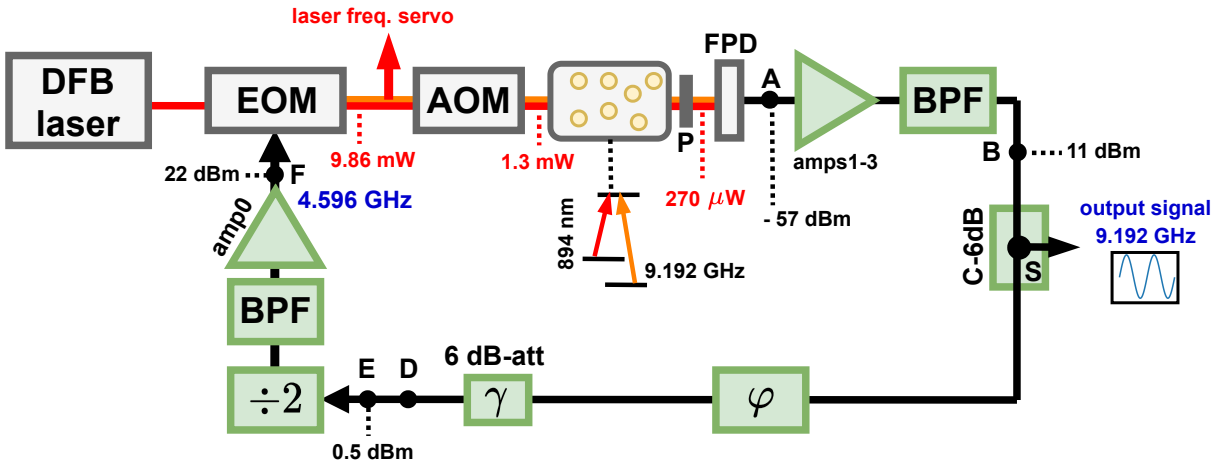

FIG. 1. (Color online) Simplified schematic of the CPT-based Cs cell feedback oscillator. The reference of the oscillator loop consists of the atomic resonance produced in the vapor cell through CPT spectroscopy. At the cell output, the resonance is detected by a fast photodiode, amplified, filtered with a band-pass filter (BPF), frequency-divided by 2 and again amplified to drive the EOM that modulates the DFB laser. Microwave isolators were used in the setup but are not shown here for clarity. The AOM is used to shift the laser frequency and control the laser power. An inset shows the CPT diagram. A linear polarizer (P) is inserted right after the cell to align respective polarizations involved in the PPOP scheme along a single axis and make possible the detection of the microwave beatnote. The typical power values at different points of the system are given for information.

back loop at 4.596 GHz, such that both first-order optical sidebands produce the CPT state. The EOM is temperature stabilized and the EOM is biased at the dark point such that the optical carrier at the EOM output is strongly reduced. At the output of the EOM, a fraction of the light is extracted and directed to an evacuated Cs vapor cell (not shown on Fig. 1 for clarity) that can be used for laser frequency stabilization using dual-frequency sub-Doppler spectroscopy[27,28]. The light propagates then into an acousto-optical modulator (AOM), driven with a radiofrequency signal at 122 MHz (−1-order). The AOM is used to compensate for the optical frequency shift induced by buffer gas in the CPT cell and for control of the laser power. The 1-cm diameter laser beam is then sent into the CPT cell, filled with 15 Torr of a N_2-Ar buffer gas mixture ($P_{Ar}/P_{N_2} = 0.6$). For tests where a static magnetic field was applied, the CPT interaction was produced with the push-pull optical pumping (PPOP) scheme[29,30]. The CPT-induced microwave resonance at the cell output is detected by a fast photodiode (FPD). The microwave resonance (A) is then first amplified by three serial amplifiers with a total gain of about 70 dB and band-pass filtered (bandwidth < 50 MHz). A phase shifter is then placed to ensure the Barkhausen phase condition of the oscillator loop. At the phase shifter output, the 9.192 GHz signal is attenuated by 6 dB, frequency-divided by 2, band-pass filtered and again amplified in order to drive the EOM at 4.596 GHz. We note that the frequency divider (Hittite HMC361) acts as an amplitude limiter, yielding for a large input power range (E) to a power of 22 dBm to drive the EOM. A 6-dB microwave coupler is placed right after the amplification stage (B) to extract the output microwave signal from the oscillator for analysis (S).

In a first step, we have measured some characteristics of the oscillator system in open-loop configuration using a network analyzer. For this, the loop is opened between points E and D. The signal from the port 1 of the analyzer is injected in the frequency divider (E), with a power of about 0.5 dBm and the output of the 6-dB attenuator (D) is connected to the port 2 of the analyzer. Figure 2 shows an example of the total gain and phase (S_{21} parameter) of the system, for a total laser power entering the cell of 1.3 mW and no static mag-

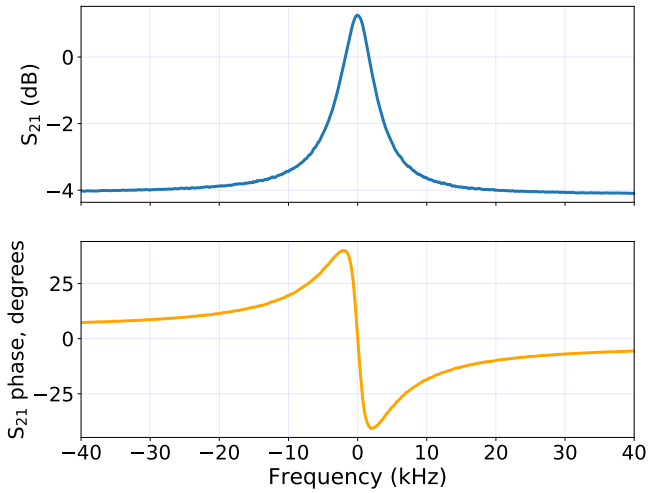

FIG. 2. Total gain and phase (S_{21} parameter, magnitude and phase) of the system, measured with a network analyzer in open loop configuration (input: E, output: D). The center of the frequency axis corresponds to an atomic resonance frequency $\nu_0 \sim 9.192640$ GHz, shifted from the exact Cs clock transition frequency due to the presence of buffer gas in the cell. A 100-pt averaging was applied onto the data.

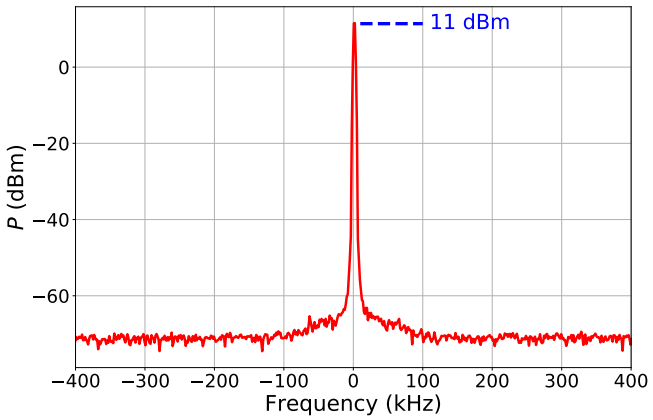

FIG. 3. Output spectrum of the CPT atomic feedback oscillator, measured at point B, for a laser power in the cell of 1.3 mW. The resonance occurs at the frequency of about 9.192640 GHz. Parameters of the analyzer are: RBW = 3 kHz, VBW = 100 Hz, sweep time = 0.2 s.

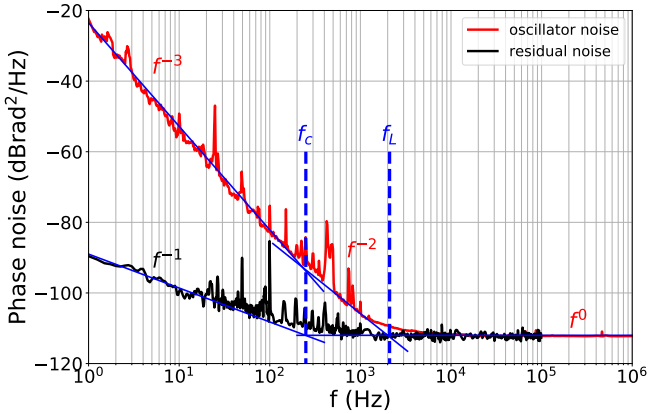

FIG. 4. Absolute phase noise at 9.192 GHz of the Cs cell atomic feedback oscillator (red line) and residual phase noise of the sustaining loop (black line). The measured Leeson frequency f_L is about 2.1 kHz, slightly lower than the calculated one $f_L = \nu_0/2Q_L$ = 2.8 kHz. The transition from the f^{-3} to the f^{-2} slope is obtained around the corner frequency f_c of the residual noise.

netic field applied. The total gain G of the system is at resonance 1.3 dB, slightly above the required oscillation condition $G = 0$ dB. The loaded Q-factor Q_L of the atomic resonator, defined as $Q_L = \frac{1}{2}\frac{d\varphi}{d\nu_0}\nu_0$, with $\frac{d\varphi}{d\nu_0}$, the resonance frequency discriminator-based phase-frequency slope and ν_0 the resonance frequency ($\sim$ 9.192640 GHz), is here 1.6×10^6.
Following these tests, we have performed some closed-loop tests and started the self-sustained oscillation by satisfying the Barkhausen conditions. Figure 3 shows the microwave signal obtained at the 6-dB coupler input (B), extracted from a measurement performed with a spectrum analyzer at the point S. The microwave power at (B) is about 11 dBm.

For further analysis, we have measured the absolute phase noise performances of the Cs-cell feedback oscillator. Results, shown on Fig. 4 for a laser power of 1.3 mW at the cell input and null static magnetic field, are completed by the measurement of the residual phase noise of the total system. The latter is the phase noise of all the components of the loop, except the Cs cell, measured separately, in the same conditions as in the oscillator, using a standard mixer-based phase detection scheme. The white phase noise is of $-$ 112 dBrad^2/Hz, in agreement with the expected value $S_{\varphi_0} = \frac{FkT}{P_A}$, where F (5 dB) and P_A (-57 dBm) are the noise figure and input microwave power of the amplification stage respectively, and kT is the thermal energy[31]. For offset frequencies $f < f_c$, with $f_c \simeq 250$ Hz here, the spectrum exhibits a phase flicker noise f^{-1} slope, yielding -90 dBrad^2/Hz at f = 1 Hz. We suspect that the main contribution of the system residual phase noise is the EOM stage, that includes the by-2 divider, the high-power 4.6 GHz amplifier and the EOM. We have measured the residual noise of the arm composed of the by-2 divider and high-power 4.6 GHz amplifier, at the level of about -105 dBrad^2/Hz at f = 1 Hz, well below the detection limit of the setup. However, its conjunction with the EOM always led, in a reproducible way, to about -90 dBrad^2/Hz at f = 1 Hz. This degradation is not fully understood yet. We found in the literature measurements of EOMs with lower residual phase noise[32] but also some with worse performances[33]. The contribution of the photodetection stage (photodiode + 3 serial microwave amplifiers at 9.192 GHz) was measured well below the total detection limit, at the level of $-$ 108 dBrad^2/Hz at f = 1 Hz.

The absolute phase noise of the Cs cell oscillator is measured in good agreement with the Leeson effect[25,26]. The phase noise spectrum is well-described by the power-law $S_\varphi(f) = \sum_{i=-3}^{0} b_i f^i$, with coefficients $b_0 = -112$ dBrad^2/Hz, $b_{-2} = -45$ dBrad^{2}Hz and $b_{-3} = -24$ dBrad^{2}Hz^2, respectively. The associated fractional frequency stability is a flicker frequency noise of $2\ln 2\frac{b_{-3}}{\nu_0^2} = 8 \times 10^{-12}$. These performances represent an important advance for CPT oscillators, since they are at least one order of magnitude better than those described in Refs[15,18,19]. However, at the present state, they are not yet at the level of state-of-the-art sapphire oscillators[34], delay-line[24] and micro-resonator-based OEOs[35] or standard CPT clocks[5,7,8].
The main limitation of the present approach is represented by the phase fluctuations induced by the sustaining loop, in particular the EOM stage, that are directly converted into frequency noise through the CPT oscillator loop. Also, the floor is limited by the low microwave power available at the input of the first amplifier following the photodetection stage. Below the Leeson frequency, this floor is converted into white frequency noise (WFN) whose level is $b_{-2} = -45$ dBrad^{2}Hz, corresponding to a fractional frequency stability of 4×10^{-13} at 1 s, a level comparable to those demonstrated by state-of-the-art CPT clocks[5,7,8]. Notice that the WFN level is due solely to fundamental quantities, like signal-to-noise ratio of the resonance and the Leeson frequency, i.e. atomic quality factor, and sets the ultimate limit of the CPT oscillator once other technical noises, like the one from the EOM stage, are made negligible. Several approaches might be

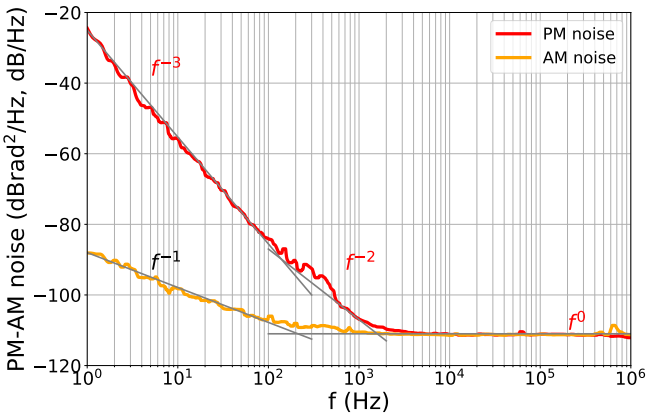

FIG. 5. AM noise and phase noise of the Cs cell feedback oscillator, measured simultaneously under identical conditions. Spurious removal was performed by the noise analyzer.

explored to improve the current oscillator performances, including the use of high-power photodiodes[36] to increase the level of microwave power and then reduce the phase noise floor, the reduction of phase fluctuations of the loop or, at the condition of detecting a powerful-enough signal, the application of a static magnetic field to increase the resonance Q-factor and then reduce the Leeson frequency. We have also started the oscillation onto the Cs atom 0-0 transition, with application of a static magnetic field. In this case, a degradation of the oscillator phase noise by about 5 dB for $5 < f < 1000$ Hz and up to 10 dB for the noise floor was observed, explained by the reduction of the number of atoms involved in the magnetic-insensitive 0-0 transition and therefore by a reduction of the resonance signal. Degradation of CPT-based oscillator performance was also observed in this case in previous studies[18,19]. We also did some tests at null magnetic field using circularly-polarized light. With similar experimental parameters, phase noise results comparable with those obtained with PPOP were obtained.

In a last part, we have performed the measurement of the AM noise of the cell-based oscillator. Corresponding results, extracted from a second measurement campaign with comparable conditions to those described in Fig. 1, are shown in Fig. 5. AM and PM noise spectra were simultaneously acquired with a phase noise analyzer (Rohde-Schwarz FSWP). We note first that the oscillator phase noise is similar to the one shown in Fig. 4. The AM noise spectrum shows a noise floor comparable to the phase noise floor, as expected since noise floors result from an additive noise mechanism, and a flicker of amplitude with $S_\alpha = 2 \times 10^{-9}/f$.
The absence of a visible Leeson effect on the AM noise spectrum is well explained by the formalism developed in Ref.[37], and is due to the frequency divider, acting as a hard amplitude limiter. Because of the divider, the output amplitude of the chain that drives the EOM is a constant, independent of the input amplitude. Thus, the gain of the amplifier chain is inversely proportional to the input amplitude, and the slope of the normalized gain $-\gamma$, defined in Ref.[37], is -1. With $\gamma = 1$, the amplitude-noise transfer function, described in Eq. 68 of Ref.[37], equals 1.
The physical meaning of the Leeson effect is that the oscillator integrates the phase fluctuations circulating in the feedback loop. The same happens with gain fluctuations, with the obvious difference that saturation prevents the amplitude from diverging. In our case, unlike "regular" oscillators and lasers, the behavior of the oscillation amplitude depends mainly on the saturation induced by the divider, which breaks the integration process mentioned above. The Leeson effect is then not visible on the AM noise and the AM noise is determined by the divider, the EOM and the microwave amplifier that follows. The AM noise of the oscillator then contains only white and $1/f$ processes. Not surprisingly[31], the AM flicker corner of the amplification chain is quite similar to that of phase noise.

In conclusion, we have reported the characterization of a microwave feedback oscillator that uses an optically-excited buffer gas-filled vapor cell as a resonator. In this approach, the microwave atomic resonance induced by CPT is detected by a fast photodiode at the cell output and maintained by a sustaining amplifier stage that feeds back an electro-optic modulated laser through a frequency divider. The phase noise of the Cs cell atomic feedback oscillator is -24, -82 and -112 dBrad^2/Hz, for offset frequencies of 1 Hz, 100 Hz and 10 kHz, respectively. These results are in good agreement with the Leeson model, with a noise floor limited by the low detected microwave power and a stability level at 1 s currently degraded by the flicker phase noise of the EOM stage converted into frequency fluctuations of the oscillator loop. In addition, we have measured the AM noise of the cell-based oscillator. The latter exhibits for $f < 200$ Hz a $1/f$ slope and a noise floor comparable to the phase noise floor. The absence of a visible Leeson effect onto the AM noise spectrum was explained by the presence of a divider in the loop acting as a hard amplitude limiter.

ACKNOWLEDGMENTS

This work has been partly funded by Conseil Régional Bourgogne Franche-Comté with the HACES project (grant 2018-04768), and in part by Agence Nationale de la Recherche (ANR) in the frame of the LabeX FIRST-TF (Grant ANR 10-LABX-48-01) and EquipX Oscillator-IMP (Grant ANR 11-EQPX-0033) projects. This work has been supported by the EIPHI Graduate school (Grant ANR-17-EURE-0002).

DATA AVAILABILITY STATEMENT

The data that support the findings of this study are available from the corresponding author upon reasonable request.

[1] G. Alzetta, A. Gozzini, L. Moi and G. Orriols, An experimental method for the observation of r.f. transitions and laser beat resonances in oriented Na vapour, Nuovo Cimento B **36,** 5-20 (1976).

[2]E. Arimondo, Coherent population trapping in laser spectroscopy, Prog. Opt., **35,** 259-354 (1996).

[3]R. Wynands and A. Nagel, Precision spectroscopy with coherent dark states, Appl. Phys. B, **20**, 1-25 (1999).

[4]J. Vanier, Atomic clocks based on coherent population trapping: a review, Appl. Phys. B Lasers Opt. **81,** DOI: 10.1007/s00340-005-1905-3 (2005).

[5]P. Yun, F. Tricot, C. E. Calosso, S. Micalizio, B. Francois, R. Boudot, S. Guérandel and E. de Clercq, High-performance coherent population trapping clock with polarization modulation, Phys. Rev. Applied **7,** 014018 (2017).

[6]X. Liu, E. Ivanov, V. I. Yudin, J. Kitching and E. A. Donley, Low-drift coherent population trapping clock based on laser-cooled atoms and high-coherence excitation fields, Phys. Rev. Appl. **8**, 054001 (2017).

[7]M. Abdel Hafiz, G. Coget, M. Petersen, C. E. Calosso, S. Guérandel, E. De Clercq and R. Boudot, Symmetric autobalanced Ramsey interrogation for high-performance coherent population- trapping vapor-cell atomic clock, Appl. Phys. Lett. **112**, 244102 (2018).

[8]P. Yun, Q. Li, Q. Hao, G. Liu, E. de Clercq, S. Guérandel, X. Liu, S. Gu, Y. Gao and S. Zhang, High-performance coherent population trapping atomic clock with direct-modulation distributed Bragg reflector laser, Metrologia **58**, 045001 (2021).

[9]P. D. D. Schwindt, S. Knappe, V. Shah, L. Hollberg and J. Kitching, Chip-scale atomic magnetometer, Appl. Phys. Lett. **85**, 26, 6409-6411 (2004).

[10]E. Breschi, Z. D. Gruji, P. Knowles and A. Weis, A high-sensitivity push-pull magnetometer, Appl. Phys. Lett. **104**, 023501 (2014).

[11]M. Bajcsy, A. S. Zibrov and M. D. Lukin, Stationary pulses of light in an atomic medium, Nature **426,** 638-641 (2003).

[12]A. Aspect, E. Arimondo, R. Kaizer, N. Vansteenkiste and C. Cohen-Tannoudji, Laser cooling below the one-photon recoil energy by velocity-selective coherent population trapping: theoretical analysis, J. Opt. Soc. Am. B **6**, 2112-2124 (1989).

[13]J. Vanier and C. Audoin, The quantum physics of atomic frequency standards, Adam-Hilger, vol. 1, (1989).

[14]A. Godone, F. Levi, S. Micalizio and C. Calosso, Coherent-population-trapping maser: Noise spectrum and frequency stability, Phys. Rev. A **70,** 012508 (2004).

[15]N. Vukicevic, A. S. Zibrov, L. Hollberg, F. L. Walls, J. Kitching and H. G. Robinson, Compact diode-laser based rubidium frequency reference, IEEE Trans. Ultrason. Ferroelec. Freq. Contr. **47,** 5, 1122-1126 (2000).

[16]L. Balet, J. Haesler and S. Lecomte, VCSEL-based Raman frequency reference on Rubidium atoms, in Proceedings of 2012 European Frequency and Time Forum. 316-319 (2012).

[17]D. Strekalov, D. Aveline, N. Yu, R. Thompson, A.B. Matsko and L. Maleki, Stabilizing an optoelectronic microwave oscillator with photonic filters, IEEE Jour. Light. Tech **21,** 12, 3052-3061 (2003).

[18]A.B. Matsko, D. Strekalov and L. Maleki, Magnetometer based on the optoelectronic oscillator, Opt. Comm. **247,** 141 (2005).

[19]D. Strekalov, A. B. Matsko, N. Yu, A. A. Savchenkov and L. Maleki, Application of vertical cavity surface emitting lasers in self-oscillating atomic clocks, J. Mod. Opt. **53,** 16-17, 2469-2484 (2006).

[20]D. Strekalov, A. A. Savchenkov, A. Matsko, N. Yu, and L. Maleki, All-Optical Atomic Clock on a Chip: Progress Report, 2004 IEEE IEEE International Ultrasonics, Ferroelectrics and Frequency Control Joint 50^{th} Anniversary Conference, Montreal, Canada, pp 104–108 (2004).

[21]S. H. Yim and D. Cho, Oscillator-free atomic clock using a multimode laser, Appl. Phys. Lett. **96,** 211119 (2010).

[22]S. H. Yim and D. Cho, Optelectronic oscillator stabilized to an intra-loop atomic filter with a coherent population trapping resonance, Journ. Kor. Phys. Soc. **61,** 1, 17–21 (2012).

[23]X. S. Yao and L. Maleki, Optoelectronic microwave oscillator, J. Opt. Soc. Am. B **13**, 8, 1725-1735 (1996).

[24]M. Li, T. Hao, W. Li and Y. Dai, Tutorial on optoelectronic oscillators, APL Photon. **6**, 061101 (2021).

[25]D. B. Leeson, A simple model of feedback oscillator noise spectrum, Proceedings of the IEEE **54**, 2, 329-330 (1966).

[26]E. Rubiola, Phase noise and frequency stability in oscillators, Cambridge University Press, 2008, 20010, 2012.

[27]M. Abdel Hafiz, G. Coget, E. de Clercq and R. Boudot, Doppler-free spectroscopy on the Cs D_1 line with a dual-frequency laser, Opt. Lett. **41,** 2982 (2016).

[28]D. Brazhnikov, M. Petersen, G. Coget, N. Passilly, V. Maurice, C. Gorecki and R. Boudot, Dual-frequency sub-Doppler spectroscopy: Extended theoretical model and microcell-based experiments, Phys. Rev. A **99,** 062508 (2019).

[29]Y. Y. Jau, E. Miron, A. B. Post, N. N. Kuzma and W. Happer, Push-pull optical pumping of pure superposition states, Phys. Rev. Lett. **93**, 160802 (2004).

[30]X. Liu, J. M. Merolla, S. Guérandel, C. Gorecki, E. de Clercq and R. Boudot, Coherent-population-trapping resonances in buffer-gas-filled Cs-vapor cells with push-pull optical pumping, Phys. Rev. A **87**, 013416 (2013).

[31]R. Boudot and E. Rubiola, Phase noise in RF and microwave amplifiers, IEEE Trans. Ultrason. Ferroelec. Freq. Contr. **59**(12), 2613-2624 (2012).

[32]K. Volyansky, J. Cussey, H. Tavernier, P. Salzentein, G. Sauvage, L. Larger and E. Rubiola, Applications of the optical fiber to the generation and measurement of low-phase-noise microwave signals, J. Opt. Soc. Am. B **25**(12), 2140-2150 (2008).

[33]S. Barke, M. Trobs, B. Sheard, G. Heinzel, K. Danzmann, EOM sideband phase characteristics for the spaceborne gravitational wave detector LISA, Appl. Phys. B **98** , 33-39 (2010).

[34]E. N. Ivanov and M. E. Tobar, Low phase-noise sapphire crystal microwave oscillators: current status, IEEE Trans. Ultrason. Ferroelec. Freq. Contr. **56** , 2, 263-269 (2011).

[35]L. Maleki, The optoelectronic oscillator, Nat. Photonics **5** , 728-730 (2011).

[36]T. M. Fortier, F. Quinlan, A. Hati, C. Nelson, J. A. Taylor, Y. Fu, J. Campbell, and S. A. Diddams, Photonic microwave generation with high-power photodiodes, Opt. Lett. **38** , 10, 1712-1714 (2013).

[37]E. Rubiola and R. Brendel, A generalization of the Leeson effect, ArXiv:1004.5539v1 (2010).